OPEN EUROPEAN JOURNAL ON VARIABLE STARS
April, 2026 http://oejv.physics.muni.cz ISSN 1801-5964
DOI: 10.5817/OEJV2026-0269

THE 2025 EE CEPHEI ECLIPSE OBSERVATIONAL CAMPAIGN

González-Carballo, J.L. (coord.); Naves Nogués, R. (coord.); Martín-Velasco, J.L. (coord.); Sisto-López, N.; Salto-González, J. L.; Reina-Lorenz, E.; Locatelli, G.; Arques-Perpiñán, J. R.; Díaz-López, S.; Escartín-Pérez, A.; García de la Cuesta, F.; Martín-Saura, A.; Limón-Martínez, F.; Botana-Alba, C.; De Elías, J.; Celiá Miró, A.; Vico, X.; Coco-López, J. C.; Arranz-Heras, T.; Bros-Caton, X.; Morales-Aimar, M.; Tremosa-Espasa, L.; Casas, R.; Perales-Vich, J. M.; Agudo-Azcona, A.; González-Farfán, R.; Carrasco-López, F.; Castillo-García, R.; Benavides-Palencia, R.; Santos-Álamo, F. M.; González-Martínez, D.; Ramos-Borrego, J. M.; Sobrino-Muñoz, R.; Otazu-Porter, X.

Observadores de Supernovas (ObSN), 06010 Badajoz (Spain), observadoresdesupernovas@gmail.com

Abstract: EE Cephei is an unusual binary system in which the eclipses are produced by the transit of an opaque and precessing dust disk surrounding the secondary component. In this work, we present the results of the observational campaign coordinated by the group Observadores de Supernovas (ObSN) during the 2025 eclipse (epoch E=13). The observations, obtained through a network of 33 observers across Spain and Italy, cover more than four months of multi-filter monitoring (*B, V, Rc, Ic*, and Sloan *g', r', i'* bands). A total of 2 698 measurements were obtained. The 2025 eclipse reached a maximum depth of 1.44 mag in the V band, breaking the trend toward shallow minima observed over the last two decades and suggesting a transit through high dust column density regions of the disk. The minimum occurred at HJD 2460993.13 ± 0.07 (multi-band mean value), showing a residual *(O-C)* of +0.77 d relative to recent linear ephemerides. Periodicity analysis using the *Phase Dispersion Minimization* (PDM) method, integrating the last six eclipses (1997–2025), yields a fundamental period of 2050.56±0.83 d, consistent with the published orbital model. These results provide an updated database for the refinement of disk precession models in this system.

Keywords: Stars: individual: EE Cephei — Binaries: Eclipsing — Stars: Be, Circumstellar matter — Dust, Extinction — Photometry

1 Introduction

EE Cep is classified in the AAVSO *Variable Star Index* (VSX; Watson *et al.*, 2006) as an E-DO type variable star. These systems are defined as binaries in which long-period, long-duration occultations are caused by a circumstellar disk surrounding one of the components. Consequently, EE Cep represents an uncommon binary system whose nature has been a subject of intense study since the mid-20th century. It is located in the constellation of Cepheus at coordinates 22 09 22.75 +55 45 24.3 (J2000.0), and its quiescent magnitude is ~10.7 (V).

Originally identified as a variable by Romano (1956), it was later confirmed as an eclipsing system by Weber (1956) and Meinunger (1973). The last three decades have been marked by the research of D. Graczyk, M. Mikołajewski, C. Gałan, and D. Pieńkowski, who have led the study of the system through extensive observational campaigns. Their work has allowed for the refinement of the orbital period and the proposal of a model based on a dark, precessing dust disk surrounding an invisible star. This approach has been fundamental in explaining why each eclipse varies in depth and duration, even attempting to predict the system's behaviour in its most recent cycles.

The orbital period of this system is approximately 5.6 years, characterized by clearly identifiable primary eclipses; however, a consistent record of a secondary minimum remains elusive. According to the VSX, the primary component is a hot B5III-IV star with a very high rotational velocity. This rapid rotation induces a non-uniform surface temperature and brightness distribution due to gravity darkening—a phenomenon known as the von Zeipel effect (Pieńkowski, 2020).

The eclipses of EE Cep are unusual in several respects. First, they exhibit varying depths between cycles, ranging from approximately 0.5 to ~2.0 magnitudes in the V band. Second, there are notable fluctuations in both the duration and the morphology of the light curves. Unlike typical eclipsing binaries, the colour indices change very little during most events, suggesting that the occultation is nearly "gray." This implies that the source of variability is not a standard stellar body but likely a medium composed of large particles. The light curves tend to be asymmetric, with a shorter recovery phase compared to the initial ingress, and they often feature "atmospheric wings" likely caused by externally semi-transparent regions within the eclipsing body (Mikołajewski & Graczyk, 1999; Gałan *et al.*, 2012; Pieńkowski *et al.*, 2020). Furthermore, a model has been proposed suggesting that the eclipsing disk may possess a multi-ring structure related to planet-forming processes (Gałan *et al.*, 2010).

The currently accepted model proposes that the eclipsing object is a dark, dusty circumstellar disk centered around a low-luminosity companion. This disk is opaque at its core and semi-transparent at its outskirts, producing the "wing" effects in the eclipse evolution and causing depth variations depending on the degree of alignment with the primary star.

A key feature of this model is disk precession. As the relative orientation of the disk changes with respect to our line of sight from one cycle to the next, both the effective inclination and the projected area of the disk shift. This results in observed eclipses that vary in depth, duration, and shape. A tentative model by Gałan *et al.* (2012) suggested a precession period of ~11–12 times the orbital period, which could account for the secular variation observed in the eclipses. However, the 2014 campaign (Pieńkowski *et al.*, 2020) revealed that the predicted very deep eclipse did not occur. This suggests that the dynamics of the disk or the primary star itself may involve additional precessional or variational components that necessitate a model revision. To date, a fully satisfactory explanation for this type of dark, dusty-disk eclipsing binary remains unavailable, highlighting the urgent need for new observational data.

Beyond photometric variability, high-resolution spectroscopy during eclipses reveals variable profiles in lines such as H-alpha and Na I, indicating complex structures within the disk environment and potentially non-uniform composition and density. Additionally, two "blue maxima" have been detected in the colour indices before and after certain photometric minima. These are interpreted as differential occultation effects, where the hotter polar regions are eclipsed differently than the cooler equatorial regions of the rapidly rotating B5 star (Gałan *et al.*, 2012).

Currently, only a few eclipsing systems are known where the occultation is caused primarily by a dust disk. The AAVSO VSX catalogs just ten such systems (E-DO), including EE Cep. Examples have been found in both evolved systems (OGLE-LMC-11893 and OGLE-LMC-ECL-17782) and pre-main sequence objects (e.g., V582 Mon and V718 Per). Among the former, ε Aurigae is the most prominent, featuring an extremely long period (~27 years) and traditionally serving as the prototype of this class. Its visible primary is an F0 Ia/Iab supergiant, and its two-year-long eclipses are attributed to a secondary object enshrouded in a dusty disk. As with EE Cep, the nature of the secondary and the disk's internal structure

DOI: 10.5817/OEJV2026-0269

remain topics of ongoing research. Recently, a new member of this class, ZTF J185259.31+124955.2, was added to the catalog (Bernhard & Lloyd, 2024).

In this context, the Observadores de Supernovas (ObSN)[1] is a Spanish group of observers dedicated to the monitoring of transient phenomena, with a primary focus on novae, supernovae, and variable stars. Over more than ten years of activity, the group has monitored numerous objects, participating in several Professional-Amateur collaborations that have resulted in co-authorship of multiple papers in peer-reviewed journals. Given that the predicted 2025 eclipse of EE Cep was set to occur when the system was favorably positioned at our latitudes, an observational campaign was organized. More than 30 observers from the group joined the effort, all of whom are located in Spain and Italy. Notably, a few group members had previously participated in EE Cep past campaigns coordinated by professional astrophysicists (Gałan *et al.*, 2012; Pieńkowski *et al.*, 2020).

The primary objective of this work is to present our observational results of the EE Cep 2025 eclipse and to make these data available to the astronomical community.

2 The observational campaign: observers and methodology

In mid-summer 2025, the ObSN coordinators proposed an intensive observational campaign to the group members regarding the imminent eclipse of EE Cep. As previously noted, a few participants had gained experience during prior events in 2009 and 2014 (Gałan *et al.*, 2012; Pieńkowski *et al.*, 2020). The response from ObSN was both immediate and enthusiastic; consequently, preparations were set in motion to begin coordinated monitoring of this eclipsing binary starting in late August 2025.

The decision was supported by the favorable meteorological conditions of the Iberian Peninsula, characterized by a high annual frequency of clear nights, as well as the optimal placement of EE Cep in the local sky during that season. With the exception of the final month of the campaign, the target remained at an altitude above 30° at the beginning of the night, thereby facilitating consistent photometric tracking and minimizing airmass concerns (Figure 1, next page). Furthermore, the geographic distribution of a large group of observers ensured data acquisition nearly every night, regardless of localized weather disruptions.

To streamline the campaign, a dedicated web portal was established[2]. This platform provided observers with essential resources, including star charts for locating EE Cep and its comparison stars, the multi-band photometric sequence to be employed, data submission forms, and interactive light curves that were updated daily as new measurements arrived.

A total of 33 observers participated in the campaign (32 based in Spain and one in Italy, Figure 2, next page). While the majority utilized private observatories and possessed extensive experience in photometry, several remote observatories located in Spain and the United States were also employed. As detailed in Appendix A, the telescopes ranged in aperture from 0.15-m to 0.35-m, all equipped with tracking mounts. Most observers utilized CCD cameras, though some employed CMOS technology for image acquisition.

All participants used photometric filters—predominantly Johnson/Cousins *B, V,* R_C, I_C—though a significant number of observers within our group also utilized Sloan (*g', r', i'*) filters.

[1] www.obsn.es
[2] https://www.obsn.es/eecep

DOI: 10.5817/OEJV2026-0269

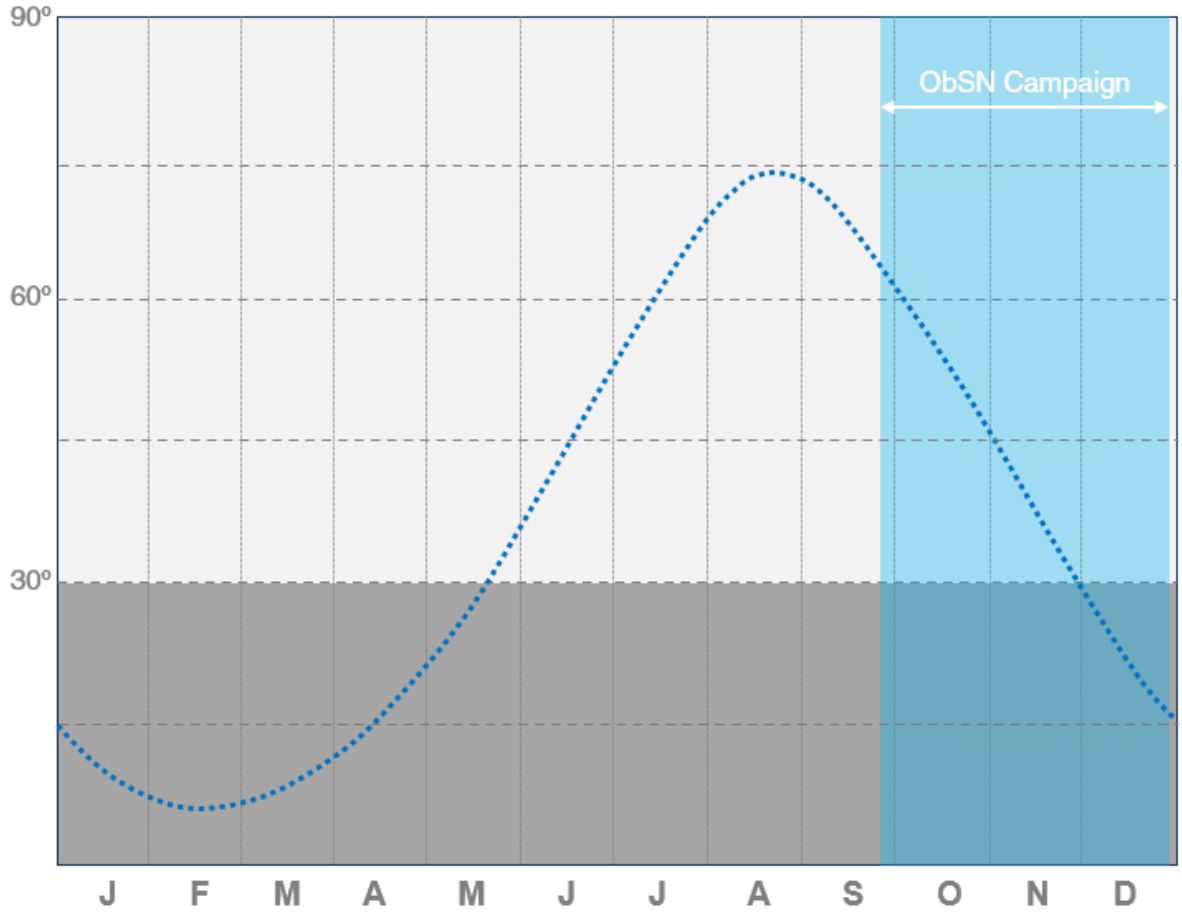

Figure 1. Monthly altitude (visibility) of EE Cephei at midnight from the central Iberian Peninsula (lat. 40° N) during 2025. The shaded grey area indicates altitudes below 30°, while the blue box highlights the duration of the ObSN Campaign

Figure 2. Geographical distribution of the observers in the ObSN's 2025 EE Cephei campaign.

http://oejv.physics.muni.cz ISSN 1801-5964
DOI: 10.5817/OEJV2026-0269

Given that EE Cep is a bright star, achieving an adequate signal-to-noise ratio (SNR) was straightforward. However, we emphasized—and conducted periodic reviews of—the importance of maintaining the linearity regime of the sensors to prevent saturation of the target star. Barring a few specific instances, the image quality consistently allowed for high-precision photometry.

Observers calibrated their frames using at least dark and flat-field corrections using specialized commercial and open-source software such as *MaximDL* (Diffraction Limited, 2012), *Astroart* (MSB Software, 2021), ASTAP (Cuypers *et al.*, 2021), or *Tycho Tracker* (jhjh) To ensure consistency in the photometry, we coordinated the use of *FotoDif* (Castellano, 2018), a well-regarded software with decades of proven reliability, frequently used by the Spanish variable star and exoplanet community.

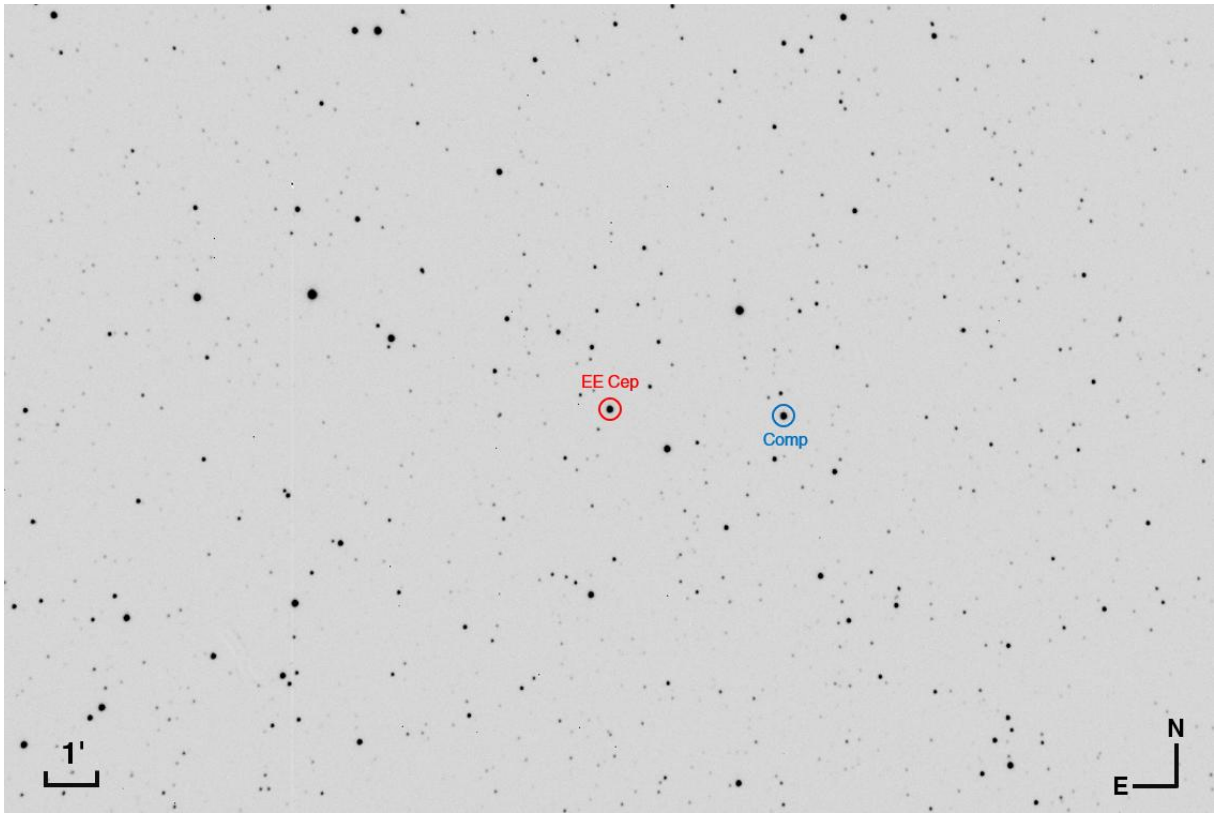

Figure 3. Star field showing the target and comparison stars (image taken by J.L. Martín, November 2, 2025. *V* filter, 30-sec. exposure).

The data uploaded to our database consisted of differential photometry relative to a single comparison star. The selection of this reference star proved challenging. Initially, we adopted the chart and photometric sequence proposed by Gałan (2014) and Pieńkowski (2020) for the 2014 campaign, which offered a handful of stars of similar magnitude in close proximity to EE Cep. Despite lingering suspicions regarding the potential variability of some candidates, we initially selected "a" star (BD+55 2690). However, shortly after the campaign began, the AAVSO reported that this star had been identified as a Delta Scuti (DSCT) variable[3].

[3] https://forums.aavso.org/t/ee-cep-strong-indication-that-comp-104-is-slightly-varying/3272

OPEN EUROPEAN JOURNAL ON VARIABLE STARS
http://oejv.physics.muni.cz
DOI: 10.5817/OEJV2026-0269
ISSN 1801-5964

Although its amplitude and period were minimal (0.02 mag and 0.0573 d, respectively) and unlikely to significantly skew our results, we opted to switch to star "b" (GSC-3973 2150). This necessitated the reprocessing of all prior data. Subsequently, "b" star was also identified as a low-amplitude (0.02 mag) Slowly Pulsating B-type (SPB) star with a period of 2.1971 d. Since over a month of monitoring had already elapsed when this was confirmed, and given we evaluated the potential impact of the variability of “b” star by inspecting residuals and intra-night scatter, confirming that it does not affect the scientific conclusions, we maintained star "b" as the photometric reference (Figure 3, previous page).

The photometric sequence for star "b" was sourced from the *ATLAS2 Catalog* (Tonry *et al.*, 2018), as it provided values across all bands used in this study (*B, V,* R_C, I_C, and Sloan *g', r', i'*. Table 1).

Table 1. Photometric Sequence of the Comparison Star

B	11.478
V	11.274
R_C	11.159
I_C	11.030
Sloan *g'*	11.288
Sloan *r'*	11.295
Sloan *i'*	11.405

Regarding data quality, the photometric error analysis shows a contained dispersion throughout the entire campaign. The internal uncertainties for individual measurements present a mean error of 0.0091 mag. By band, the mean error stands at 0.0103 for *B*, 0.0086 for *V*, 0.0092 for R_C, and 0.0099 for I_C. In the Sloan filter system, the recorded mean errors were 0.0075 (g'), 0.0076 (r'), and 0.0108 (i'). These uncertainties indicate that the detected structures in the light curve, such as the plateaus during ingress and the variations in color indices, are statistical significance and are not the result of instrumental noise or unfavorable atmospheric conditions (Figure 4).

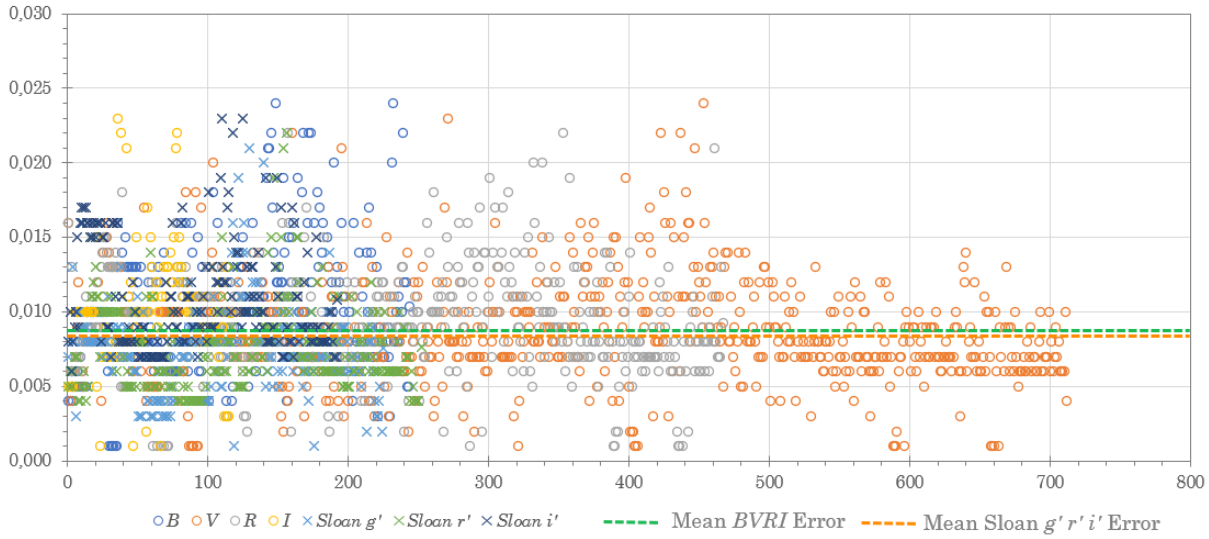

Figure 4. Internal uncertainties for each individual measurement and band.

DOI: 10.5817/OEJV2026-0269

The campaign commenced on August 22, 2025 (HJD 2460910), approximately five weeks prior to the predicted start of the eclipse, and continued until several weeks after the star had recovered its out-of-eclipse brightness. The final measurement was recorded on December 28, 2025 (HJD 2461038). Over the course of 128 days, we obtained data nearly every night, with the exception of a few dates when poor weather conditions affected the entirety of Southern Europe. In total, 2 698 measurements were collected.

3 Campaign results: The 2025 eclipse of EE Cep

Following the nomenclature established in literature and previous international observational campaigns (Mikołajewski *et al.*, 2005; Pieńkowski *et al.*, 2020), the event recorded in 2025 is identified as the epoch E=13 eclipse. This numbering is based on the reference linear ephemeris, which sets the origin (E=0) at the minimum observed in 1952 (HJD 2434344.1). The correct cataloging of the current eclipse as the thirteenth cycle in the historical series allows for a direct comparison of the residuals *(O-C)* and the morphological evolution of the circumstellar disk over a 73-year time horizon. This facilitates the integration of our observations into the long-term depth variation and precession models proposed for this binary system.

3.1 Results

Our observational campaign for the monitoring of the 2025 eclipse of EE Cep spanned a period of over 4 months (128 days), starting in late August 2025 (HJD 2460910), approximately 83 days before the minimum, and concluding in late December of the same year (HJD 2461037), about 45 days after the minimum. It should be noted that, as mentioned in the previous section, although the initial goal was to extend the monitoring during the late egress, the campaign had to be terminated due to a succession of Atlantic fronts that swept across the Iberian Peninsula (and northern Italy) in the following weeks.

This time window allowed for comprehensive coverage, documenting the phases from the early atmospheric ingress to the partial recovery of brightness following the maximum occultation phase. As previously noted, 2 698 measurements were submitted to our database.

Owing to the diverse geographical locations of the participating observers, measurements were resulted in near-continuous coverage. The distribution of measurements by band shows a balanced spread that ensures the consistency of the calculated indices, with those obtained using V and R filters being notably more numerous (29.1% and 19%, respectively). Additionally, 33% of the measurements were obtained using Sloan *g', r',* and *i'* filters (Figures 5, next page).

The availability of multi-filter data has not only guaranteed a precise characterization of the light curve but has also enabled us to calculate colour indices (B-V, R-I_C, etc.), as will be discussed further on.

http://oejv.physics.muni.cz
DOI: 10.5817/OEJV2026-0269 ISSN 1801-5964

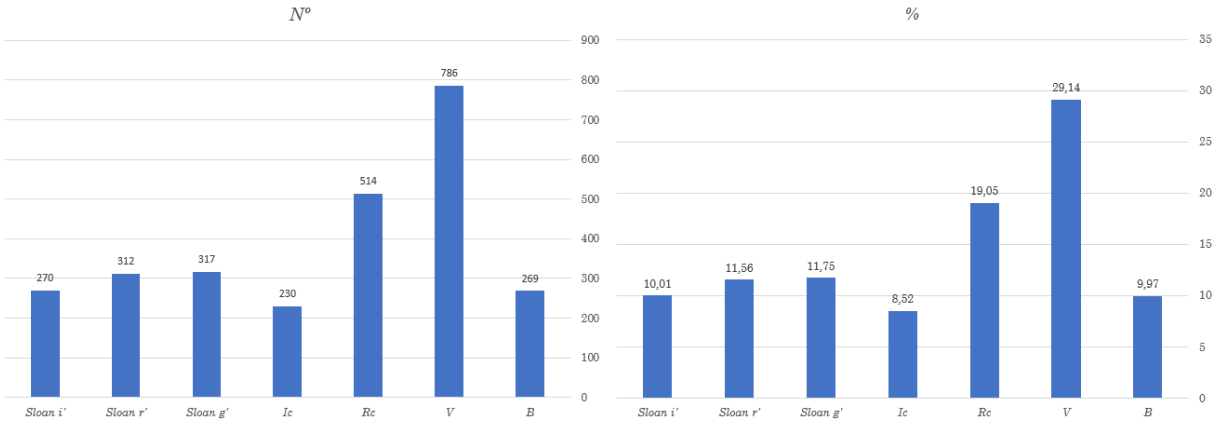

Figure 5. Distribution of campaign measurements by band, showing total counts and relative percentages.

3.2. Photometric evolution and characterization of the EE Cep 2025 Eclipse

We present below a description of the behaviour of the 2025 eclipse of EE Cep, as well as a preliminary analysis of the results obtained. This analysis does not intend to be exhaustive, but rather to show its evolution and main characteristics in comparison with previous eclipses.

As previously mentioned, the photometric variability of EE Cephei is associated with the occultation of an early-type primary star by a secondary object surrounded by an opaque and precessing circumstellar dust disk. The morphology of its light curves shows a critical dependence on the disk inclination, as well as the minimum projected distance between the centers of both components on the visual plane. Based on the literature regarding the events produced over the last 70 years, it is shown that the system has exhibited eclipses with widely varying depths and behaviours; thus, records between 1947 and 2020 show a range of amplitudes oscillating between ~0.5 magnitudes (as in the eclipses of 1969, 2003, 2009, and 2020) and ~2.0 magnitudes (as in 1958 and 1964). The most recent events, specifically those of 2003, 2009, 2014, and 2020, were characterized by being especially shallow, with drops of 0.6, 0.5, 0.71, and 0.55 magnitudes in the V band respectively, which appeared to indicate a gradual decrease in eclipse depth.

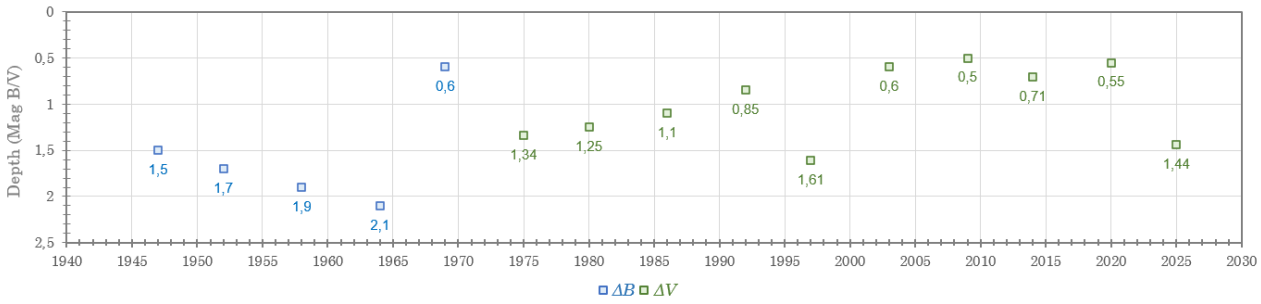

Figure 6. Evolution of eclipse depths of EE Cep from 1957 to 2025 (adapted from Pieńkowski *et al.*, 2020).

The 2025 eclipse has shown a behaviour that breaks this trend of shallow, low-opacity eclipses of the last two decades (Figure 6, previous page). According to the observations

OPEN EUROPEAN JOURNAL ON VARIABLE STARS
http://oejv.physics.muni.cz
DOI: 10.5817/OEJV2026-0269
ISSN 1801-5964

obtained, the system reached a maximum depth of 1.44 magnitudes in the V band. This amplitude is significantly greater than that recorded in the previous 2020 cycle (0.55 magnitudes), placing it among the deepest since records began and only surpassed by those of the 1947-1969 period and the 1997 event. The data seem to place the 2025 eclipse in a high dust column density regime, similar to the levels observed in 1975 or 1997 (1.34 and 1.61 magnitudes in the V band, respectively).

In this regard, Figure 7 shows a comparison of the 2025 eclipse with the immediately preceding ones (2003, 2009, 2014, and 2020; source: *AVSO International Database*) by superimposing the light curves, aligned from the date of the minimum. This allows us to visualize that the 2025 eclipse has represented a change in trend compared to the previous ones: while the events of the beginning of the century are grouped in the low-amplitude zone, the 2025 curve deviates visibly, creating a much sharper and deeper profile and, therefore, exhibiting a more pronounced recovery phase towards its baseline brightness.

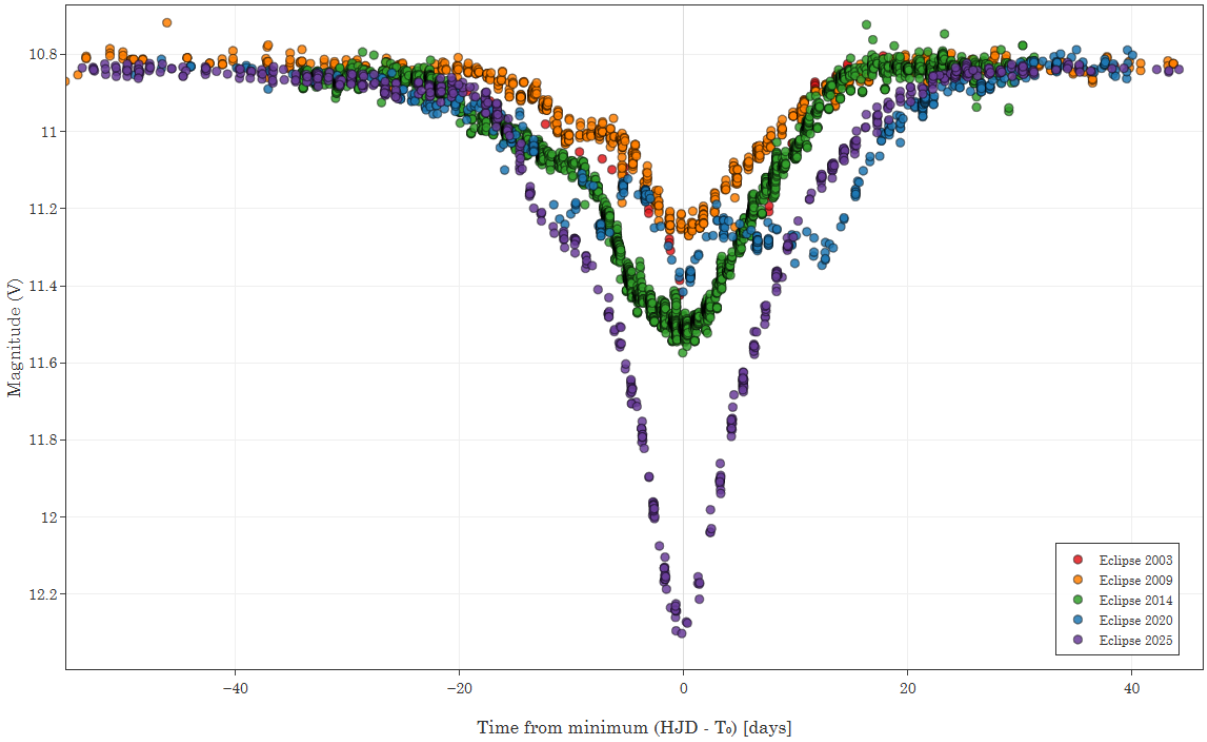

Figure 7. Superimposed light curves of the last five eclipses of EE Cep (*E=9* to *13*), aligned by their minima. Data for *E=9* to *12* were obtained from the *AAVSO International Database* (Kafka, 2021).

The photometric evolution of the 2025 eclipse observed from the data obtained in our campaign can be seen in Figure 8 (next page), which represents all measurements obtained in different bands. This cycle E=13 has been characterized by a truncated "V" morphology, similar to that of 2014 but with less asymmetry between its descending and ascending branches and very different from the previous 2020 eclipse. Furthermore, as noted above, the eclipse was relatively deep, which can be interpreted as the transit path across the stellar disk intersecting denser and more central regions of the circumsecondary dust disk.

The eclipses of EE Cep usually fit a profile consisting of four contact moments (1, 2, 3, and 4) that delimit the phases, with specific subdivisions for the beginning and the end (1a and 4a), which seem to be due to the extended nature and opacity level of the different regions

OPEN EUROPEAN JOURNAL ON VARIABLE STARS
http://oejv.physics.muni.cz
DOI: 10.5817/OEJV2026-0269
ISSN 1801-5964

of the dust disk, as well as its precession (Graczyk *et al.*, 2003 and Gałan *et al.*, 2010). In general terms, we can observe that the 2025 eclipse has adjusted quite well to this model.

The beginning of the eclipse has always been difficult to determine. We have observed a slight oscillation around its start, consisting of a slight drop in brightness of ~0.02 magnitudes with a duration of approximately six days in all bands, followed by a rapid recovery prior to the main brightness drop, which began at HJD ~2460966 (Figure 9, next page). This slight fluctuation could well correspond to what was observed by Gałan (2012) in the 2003 eclipse as shallow minima about 35 days before and after the minimum. From there, the brightness decline began, which, although starting gradually, was constant (dropping ~0.3 magnitudes in 6 days) until reaching a bump that is perfectly documented between HJD ~2460979 and ~2460984, where the brightness drop slowed to a rate of 0.06 V mags in 6 days. This hump is perfectly visible in all bands and has been documented in previous eclipses, such as those in 2009 and 2014 (which was even more prolonged in time), also occurring about 9-10 days before the minimum and being related to the annular structure of the disk and the transition to areas of greater opacity within it (Pieńkowski *et al.*, 2020).

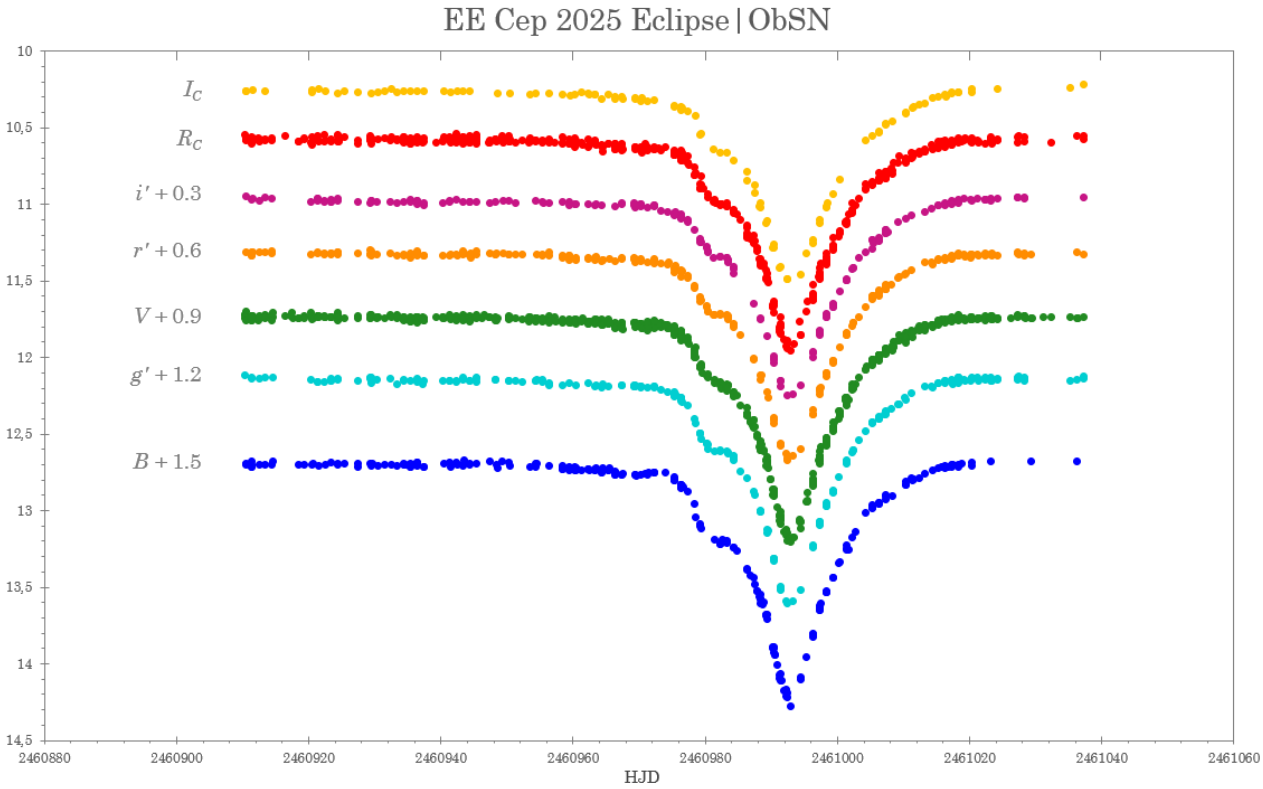

Figure 8. Multi-filter light curve of the 2025 EE Cep eclipse, including all measurements submitted during the campaign.

DOI: 10.5817/OEJV2026-0269

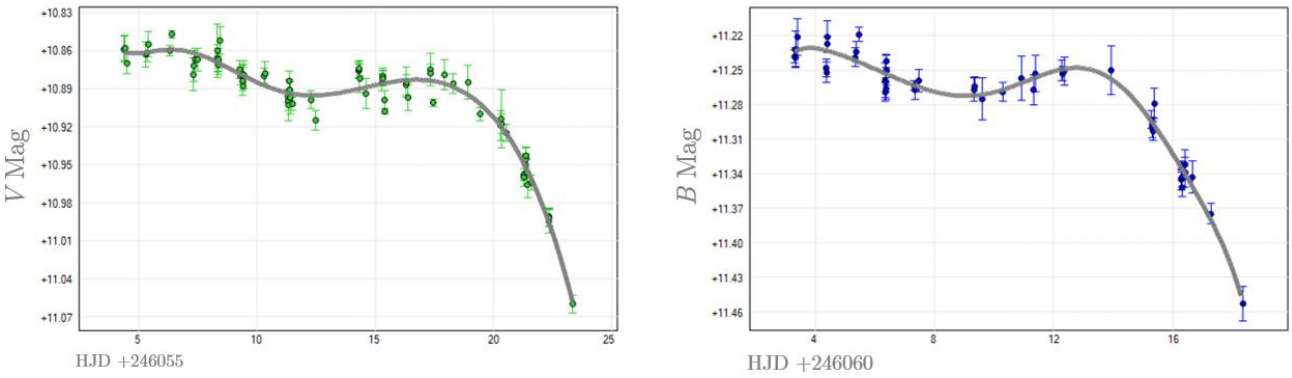

Figure 9. Detail of the eclipse ingress, showing a slight brightness dip followed by a recovery in the V and B bands.

The transit toward the point of maximum depth was, therefore, not a monotonic fall, but a process marked by these structural irregularities. The central minimum was reached around HJD 2460993.066 in the V band, with slight variations between bands that place the B, R_C, and I_C minima at HJD 2460993.115, 2460993.132, and 2460993.206 respectively. The moments of minimum and the magnitudes of minimum in the different bands used in our observational campaign can be seen in Table 2. These minima have been calculated using the Kwee-van Woerden Extremum Calculation function implemented in the *Peranso* software (Paunzen & Vanmunster, 2016), restricting the fit to the central section of the eclipse to minimize asymmetry effects.

Table 2. Observed minima epochs and magnitudes, including the eclipse depth per band.

	Minimum (HJD)	**Magnitude at minimum**	**Depth**
B	2460993.115±0.106	12.602	1.403
V	2460993.066±0.125	12.274	1.437
R_C	2460993.132±0.158	11.827	1.249
I_C	2460993.206±0.224	11.403	1.14
Sloan g'	2460992.862±0.099	12.355	1.402
Sloan r'	2460993.227±0.811	12.005	1.282
Sloan i'	2460993.202±0.113	11.889	1.203

OPEN EUROPEAN JOURNAL ON VARIABLE STARS
http://oejv.physics.muni.cz
DOI: 10.5817/OEJV2026-0269
ISSN 1801-5964

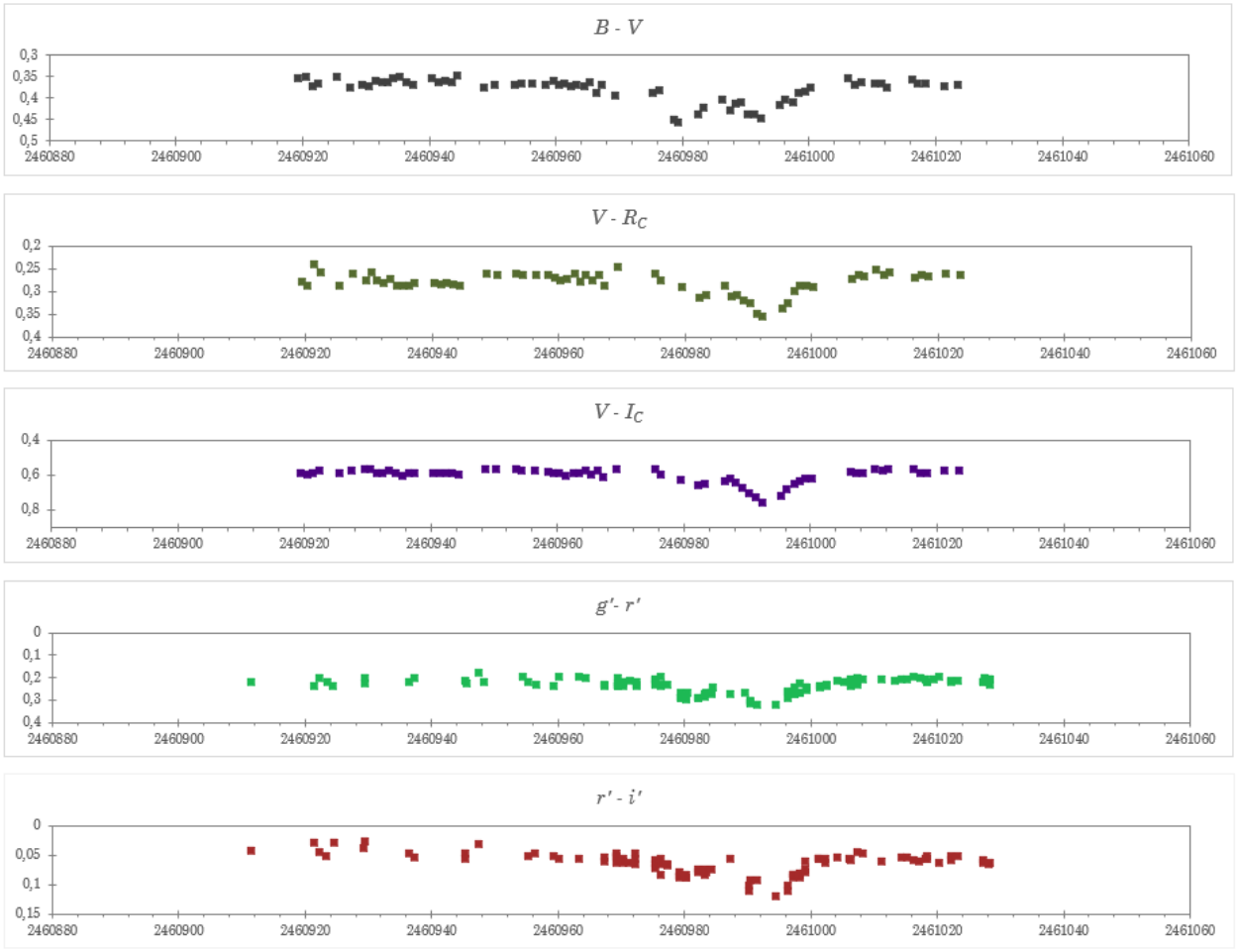

Figure 10. Evolution of color indices during the 2025 campaign. Dates are in HJD.

The recovery phase after the minimum showed an asymmetry in all bands with respect to the ingress, with a less pronounced egress slope and a return to the quiescent magnitude (~10.837 in V) that extended over a longer period than the ingress. This prolonged egress morphology is usually interpreted as an indicator of the physical extent of the outer regions of the dust disk after the passage of the center of mass of the secondary.

The behaviour of the colour indices during the 2025 event confirms the selective nature of the extinction (Figure 10). The data show a progressive increase in the B-V index from a baseline of 0.35 to a maximum value of 0.46 at the minimum, representing a reddening of 0.11 magnitudes. The V-I_C index exhibits an even more pronounced variation, passing from 0.58 to 0.76 during the phase of maximum occultation. This wavelength dependence on eclipse depth is much more evident than in 2014 (Gałan *et al.*, 2020), where low transit opacity limited the detection of significant chromatic changes. As in previous eclipses, minima are observed in the evolution of the colour indices around the hump that occurs about 9/10 days before the minimum. Overall, the amplitude of the reddening observed in 2025 can be directly correlated with the greater depth of the eclipse, consistent with extinction produced by dust with sufficient optical depth to generate a detectable chromatic signature in the visible and near-infrared spectrum.

The multi-filter photometric observations obtained during the 2025 EE Cephei eclipse campaign place the astronomical minimum in a range from HJD 2460993.066 (V filter) to

DOI: 10.5817/OEJV2026-0269

2460993.206 (I_C filter). By contrasting these values with the refined linear ephemeris proposed by Pieńkowski *et al.* (2020), converted to HJD for comparision:

$$\mathrm{JD_{min}} = 2434345.16\ (\pm\ 2.08) + 2049^{\mathrm{d}}.78\ (\pm\ 0^{\mathrm{d}}.22) \times \mathrm{E}$$

The photometric determinations presented here place the minimum between HJD 2460993.066–2460993.206 depending on the filter, with a multi-band average of HJD 2460993.13 ± 0.07. The observed offset with respect to the linear prediction is therefore $\Delta T \approx +0.77$ d for the V band. This result shows a more than acceptable coherence with the evolutionary trend of the system documented in the last three decades (Figure 11). The measured positive offset confirms the persistence of the systematic delay observed in epochs E=9, 10, and 11, where residuals stabilized around +0.75 days. This stability in the *(O-C)* suggests that the orbital period of 2049.78 days derived from recent international campaigns constitutes a robust basis for the dynamic description of the system. Nonetheless, the subtle chromatic dependence detected in the times of minimum (a difference of 0.14 days between the V and I_C filters), if instrumental systematics are negligible, evidences the structural complexity of the circumstellar disk. These data confirm that, while the orbital periodicity is predictable, the eclipse geometry remains influenced by density gradients and precession effects in the secondary component, validating the physical model discussed in recent literature.

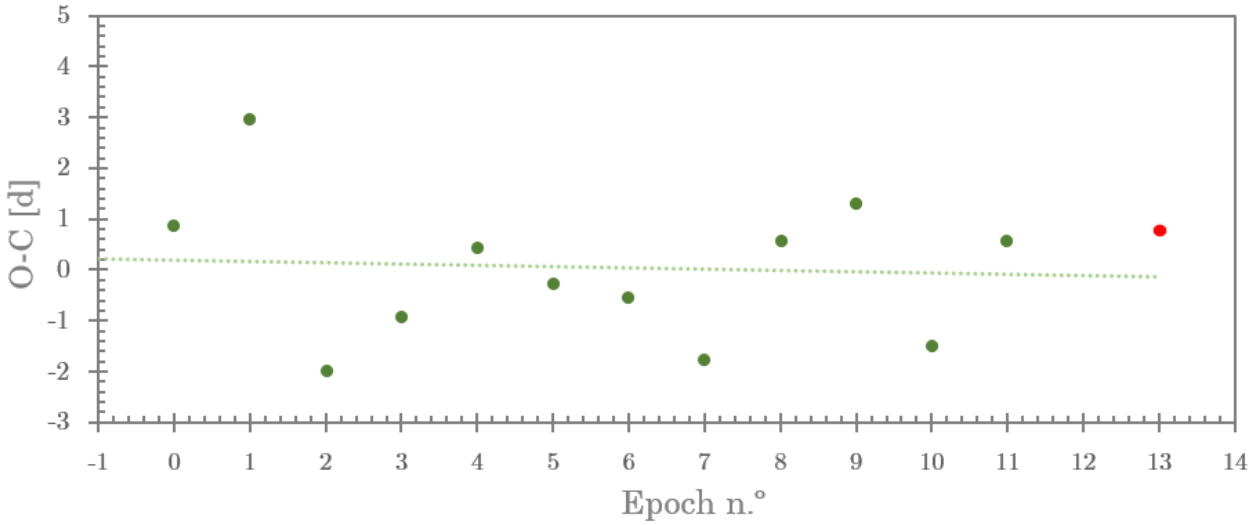

Figure 11. *O-C* diagram with linear fit (adapted from Pieńkowski *et al.*, 2020). The red dot corresponds to our derived value for the 2025 Eclipse.

To consolidate the interpretation of the E=13 cycle data in a historical context, a new determination of the orbital period has been carried out by integrating the photometry of the last six eclipses (1997-2025), using V band records from the *AAVSO International Database* for the first five events (Figure 12, next page). Given that the EE Cephei system presents narrow and deep minima separated by long intervals of quiescence, the Phase Dispersion Minimization (PDM) algorithm (Stellingwerf, 1978) has been employed, which is optimal as it is independent of the shape of the light curve. The analysis yields a fundamental period of 2050.56 ± 0.83 days (1σ uncertainty), providing a robust estimate that remains consistent with the historical baseline despite the relatively low number of cycles used in this specific PDM run.

DOI: 10.5817/OEJV2026-0269

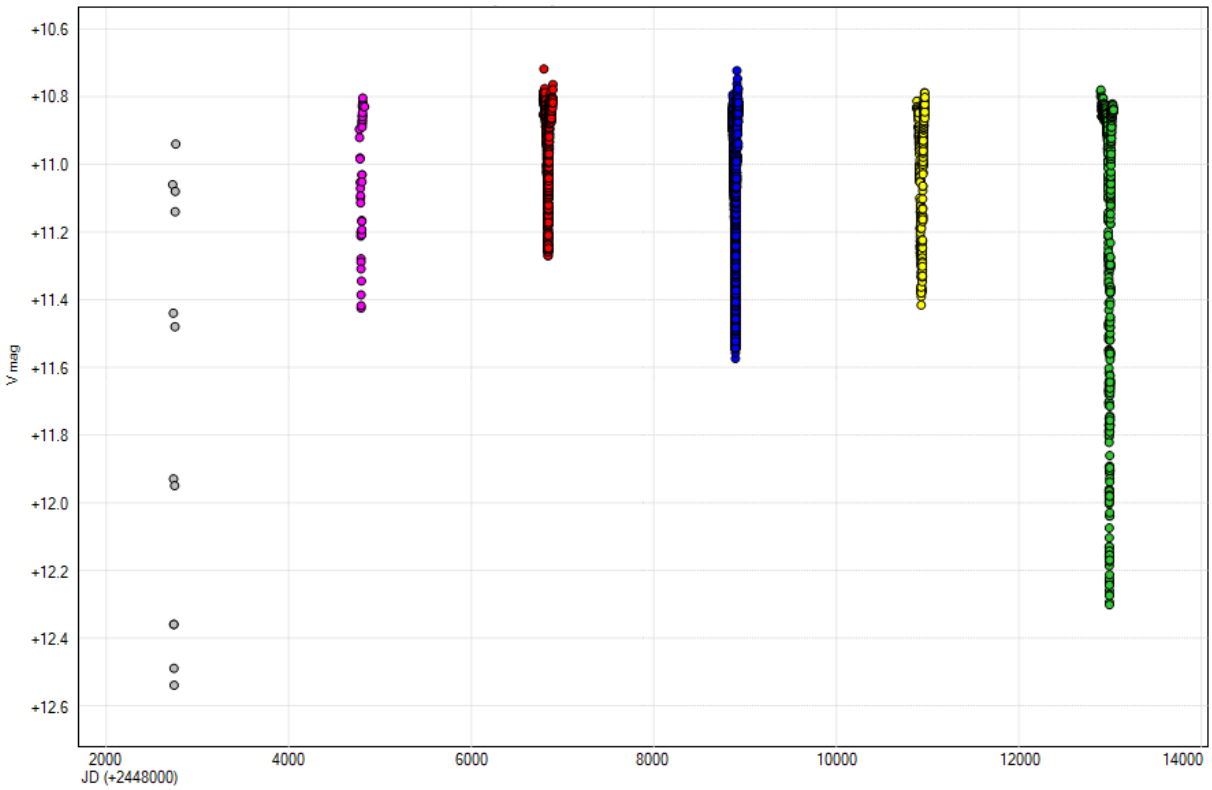

Figure 12. Last six eclipses of EE Cep (1997–2020 data obtained from the *AAVSO International Database;* green dots E=13, our data).

This result presents a robust agreement with the linear ephemeris of Pieńkowski *et al.* (2020) (P = 2049.78 ± 0.22 d) and with the historical values of 2050.44 d cited in previous literature. The convergence of the PDM toward this value, compared to spurious solutions of shorter periods obtained through harmonic methods, confirms that the kinematic structure of the system remains stable after more than three decades of monitoring. Nevertheless, the persistence of slightly positive *(O-C)* residuals in the most recent cycles suggests that the observed variations are photometric and not orbital in nature, likely linked to the morphological evolution of the circumstellar disk or to precession effects that shift the light minimum relative to the lower conjunction of the components.

4 Conclusions

The results derived from the observational campaign of the EE Cephei eclipse in 2025 (epoch E=13) reveal a significant evolution in the system's behavior. The recorded maximum depth of 1.44 magnitudes in the V band represents a clear break from the trend of shallow minima documented over the last two decades, specifically between the 2003 and 2020 cycles. This increase in amplitude suggests that the transit chord of the primary star has intercepted regions with a higher dust column density, which underscores the dynamic and changing nature of the circumstellar disk's opacity.

In terms of timing, the average time of minimum determined at HJD 2460993.13 ± 0.07 yields an (O–C) residual of +0.77 d relative to the linear ephemeris of Pieńkowski et al. (2020). The persistence of this positive offset, which has remained stable since epoch E=9, is consistent with current orbital models and suggests that the observed timing discrepancies have a

DOI: 10.5817/OEJV2026-0269

photometric origin linked to the disk geometry rather than kinematic variations of the system. Likewise, the determination of a fundamental period of 2050.56 ± 0.83 days (1σ uncertainty), obtained using the Phase Dispersion Minimization (PDM) method, reinforces the stability of the orbital period over more than seven decades of observations. However, given the limited number of cycles and the intrinsic limitations of the PDM method in estimating formal uncertainties, this error should be regarded as an approximate indicator of the period dispersion. Within this context, the result disfavors shorter period solutions, which are likely artifacts of harmonic fitting methods.

Finally, the multi-filter characterization points toward a subtle yet selective extinction, evidenced by modest reddening during the minimum and slight chromatic differences in the contact times. This relatively small selective effect supports a non-stellar origin of the obscuring body, most likely a circumstellar disk, and constitutes a key diagnostic in distinguishing EE Cephei from other variable systems. For instance, the case of V383 Sco (Gałan *et al.*, 2013) demonstrates that objects with remarkably similar eclipse morphologies can be shown to belong to fundamentally different classes once multi-band photometry is considered, particularly through the inclusion of *I*-band data. The present study not only updates the status of EE Cephei in its thirteenth documented cycle but also underscores the importance of continued monitoring to capture the intrinsic variability of this binary system.

Acknowledgements. *This research has made use of the AAVSO International Database, and we acknowledge with thanks the variable star observations contributed by observers worldwide.*

The authors are grateful to Dr. David Galadí Enríquez (Department of Physics, University of Córdoba, Spain) for his review of this work and for his valuable contributions to it.

References

Bernhard, K., & Lloyd, C., 2024, *ZTF J185259.31+124955.2: A new evolved disc-eclipsing binary system*, Astronomy & Astrophysics, 688, id.A58. 2024A&A...688A..58B

Castellano, J., 2018, FotoDif 3.95, [Computer software]. Retrieved from: http://www.astrosurf.com/orodeno/fotodif/

Cuypers, J., *et al.*, 2021, ASTAP: Astrometric Stacking Program, [Computer software]. Retrieved from: https://www.hnsky.org/astap.htm

Diffraction Limited, 2012, MaxIm DL, [Computer software]. Retrieved from: http://diffractionlimited.com/product/maxim-dl/

Gałan, C., *et al.*, 2010, *Complex structure of the disc in the EE Cephei system*, Astronomy & Astrophysics, 517, id.A15. 2010A&A...517A..15G

Gałan, C., *et al.*, 2012, *International observational campaigns of the last two eclipses in EE Cep: 2003 and 2008/9*, Astronomy & Astrophysics, 544, id.A53. 2012A&A...544A..53G

Gałan, C., et al., 2013, *A new look at the long-period eclipsing binary V383Scorpii*, Astronomy & Astrophysics, 550, id.A93. 2013A&A...550A..93G

Gałan, C., 2014, *The international campaign of the EE Cephei eclipse in 2014*, Astronomy & Astrophysics, 639, id.A2. 2020A&A...639A..23P

Kafka, S., 2021, Observations from the AAVSO International Database, American Association of Variable Star Observers, https://www.aavso.org

Meinunger, L., 1973, Mitt. Verän. Sterne, 6, 89.

Mikołajewski, M., & Graczyk, D., 1999, *Is the eclipsing variable EE Cep a cousin of ε Aur?*, Monthly Notices of the Royal Astronomical Society, 303, 521. 1999MNRAS.303..521M

DOI: 10.5817/OEJV2026-0269

MSB Software, 2021, Astroart 8.0, [Computer software]. Retrieved from: https://www.msb-astroart.com/
Parrott, D., 2020, *Tycho Tracker: A New Tool to Facilitate the Discovery and Recovery of Asteroids using Synthetic Tracking and Modern GPU Hardware*. Journal of the American Association of Variable Star Observers (JAAVSO), 48(2), 262. 2020JAVSO..48..262P
Paunzen, E. & Vanmunster, T., 2016, Peranso: Period Analysis Software, [Computer Software]. Retrieved from: http://www.cbabelgium.com
Pieńkowski, D. *et al.*, 2020, *International observational campaign of the 2014 eclipse of EE Cep*, Astronomy & Astrophysics, Volume 639, id.A23. 2020A&A...639A..23P
Romano, G., 1956, Coelum, 24, 135.
Stellingwerf, R. E., 1978, *Period determination using phase dispersion minimizatio*n, Astrophysical Journal, 224, 953-960. 1978ApJ...224..953S
Tonry, J. L., *et al.*, 2018, *The ATLAS All-Sky Stellar Reference Catalog*, Astrophysical Journal, 867, id.105. 2018ApJ...867..105T
Watson, C. L., *et al.*, 2006, *The International Variable Star Index (VSX)*, The Society for Astronomical Sciences Annual Symposium, 25, 47. 2006SASS...25...47W
Weber, R., 1956, Doc. Des Obs. Circular, no. 9.

DOI: 10.5817/OEJV2026-0269

Appendix A

Observational setup: Participating observatories and technical specifications

Observer	**Observatory**	**Location**	**Country**	**MPC Code**	**Telescope Diameter**	CCD/CMOS	**Filters**
Agudo Azcona, A.	Obs. Las Vaguadas	Badajoz	Spain		0.23-m	CCD ATIK 383L+ M	*V*
Arques Perpiñán, J. R.	Trevinca Skies	Valdin	Spain		0.12-m	ZWO ASI 2600MM PRO & ASI 533MC	*B, V, R_C,* Sloan *g', r'*
Arques Perpiñán, J. R.	Utah Desert Remote Obs.	Beryl, Utah	USA	U94	0.43-m	FLI-PL6303E	*B, V, R_C, I_C*
Arranz Heras, T.	Obs. Las Pegueras	Navas de Oro	Spain		0.35-m	Atik 460 EX	*V*
Benavides Palencia, R.	Obs. Posadas	Posadas	Spain	J53	0.35-m	QHY9 MM	*V*
Botana Alba, C.	Magalofes	Fene	Spain	Y85	0.2-m	ZWO ASI183MM Pro	*B, V,* Sloan *r'*
Bros Caton, X.	Anysllum	Àger	Spain	C07	0.35-m	ASI2600MM Pro	*V*
Carrasco López, F.	Obs. Villuercas	Navezuelas	Spain	R49	0.2-m	CMOS ZWO ASI 533MM Pro	*V,* Sloan *g', r'*
Casas, R.	Obs. L'Estartit	L'Estartit	Spain		0.20-m	CMOS Moravian C2-5000A	*V, R_C*
Castillo García, R.	Obs. Pico de San Pedro	Tres Cantos	Spain	Z83	0.25-m	SBIG ST8XME	*B, V, R_C, I_C*
Celiá Miró, A.	Obs. Albireo Inca	Crestatx-Sa Pobla	Spain	K13	0.15-m	CMOS Player One Apollo-M	*V, R_C*
Coco López, J. C.	Obs. Hypatia	Valencina de la Concep.	Spain		0.20-m	CMOS ZWO ASI 533MM Pro	*B, V, R_C, I_C, U*
De Elías, J.	Obs. Majadahonda	Majadahonda	Spain	L46	0.2-m	ZWO ASI1600MM Pro	*B, V, R_C, I_C*
Diaz López, S.	AstroCamp	Nerpio	Spain	I79	0.26-m	ZWO ASI 2600MM PRO	Sloan *g', r', i'*
Escartin Pérez, A.	IO-03 AAVBAE.net Trevinca	Bilbao	Spain		0.25-m	Moravian G2-8300 CCD	Sloan *g', r', i'*
García de la Cuesta, F.	La Vara, Valdes	Muñás de Arriba	Spain	J38	0.25-m	CCD ST8XME +AOL	*V, R_C, I_C,* Sloan *g'*
González Farfán, R.	Uraniborg	Écija	Spain	Z55	0.28-m	CCD Atik 414EX M	*V*
González Martínez, D.	Obs. Rubí	Rubí	Spain		0.20-m	ZWO ASI294mm pro	*V, R_C*
Limon Martínez, F.	Obs. Mazariegos	Mazariegos	Spain	Z50	0.20-m	ZWO ASI 533MM	*V, R_C*
Locatelli, G.	Maritime Alps Obs.	Cuneo	Italy	K32	0.30-m	QHY9	*V, R_C,* Sloan *g', r', i'*

DOI: 10.5817/OEJV2026-0269

Martin Saura, A.	Ob. Sureste Estelar	Fuente Álamo	Spain	R63	0.2-m	ZWO ASI294MM Pro	*V, R_C*
Martin Velasco, J. L.	Carpe Noctem Obs.	Collado Mediano	Spain	I72	0.3-m	SBIG ST-10XME	*B, V, R_C, I_C*
Morales Aimar, M.	Obs. de Sencelles	Sencelles	Spain	K14	0.25-m	SBIG ST-7XME	*V*
Naves Nogues, R.	Montcabrer	Cabrils	Spain	213	0.30-m	Moravian G4-9000	*V, R_C,* Sloan *g', r', i'*
Otazu Porter, X.	Obs. Lo Olivaret	Alcampell	Spain		0.28-m	CMOS Moravian C3-61000 PRO	*B*
Perales Vich, J. M.	Obs. de Llubí	Llubí	Spain		0.2-m	ZWO ASI 533MM	*B, V, R_C*
Ramos Borrego, J. M.	Obs. IES Al-Baytar	Benalmádena	Spain	R52	0.20-m	ZWO ASI294mm Pro	*V*
Reina Lorenz, E.	Obs. de Masquefa	Masquefa	Spain	232	0.25-m	CMOS Zwo ASI 294MM Pro	*B, V, R_C, I_C*
Salto González, J. L.	Cal Maciarol mòdul 8 Obs.	Àger	Spain	A02	0.3-m	CCD Moravian G4-9000	*V,* Sloan *g', r', i'*
Santos Álamo, F. M.	Obs. Giordano Bruno	Piconcillo	Spain	G05	0.20-m	CCD ATIK 420 MM	*B, V, R_C, I_C*
Sisto López, N.	El Observathorreo	O Bolo	Spain		0.1-m	ZWO ASI2600MM	*B, V, R_C, I_C,* Sloan *g', r', i'*
Sobrino Muñoz, R.	Obs. Roberto-Piriz, UCLM	Ciudad Real	Spain		0.14-m	QHY9 MM	*V, R_C*
Tremosa Espasa, L.	Obs. El Sueño	Vinyols i els Arcs	Spain	C90	0.3-m	Sbig ST8 XE	*V, R_C*
Vico, X.	Obs. Petit Sant Feliu	Sant Feliu Llobregat	Spain	D02	0.25-m	CMOS ASI 1600MMC	*B, V, R_C*